Annals of Phytomedicine 12(2): 607-619, 2023

DOI: http://dx.doi.org/10.54085/ap.2023.12.2.71

Annals of Phytomedicine: An International Journal
http://www.ukaazpublications.com/publications/index.php

Print ISSN : 2278-9839 Online ISSN : 2393-9885

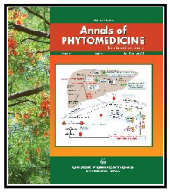

Original Article : Open Access

Empagliflozin causes nephrotoxicity in patients on guideline-directed medical therapy *via* urokinase-type plasminogen activator: An *in silico* approach

Anu Philip, Prarambh S. R. Dwivedi*, C. S. Shastry◆ and Basavaraj Utagi**

Department of Pharmacy Practice, NGSM Institute of Pharmaceutical Sciences (NGSMIPS), Nitte (Deemed to be University), Mangalore-575018, Karnataka, India

** Department of Pharmacology, NGSM Institute of Pharmaceutical Sciences (NGSMIPS), Nitte (Deemed to be University), Mangalore-575018, Karnataka, India*

*** Department of Cardiology, KS Hegde Medical Academy (KSHEMA), Nitte (Deemed to be University), Mangalore-575018, Karnataka, India*

Article Info

Article history
Received 2 July 2023
Revised 21 August 2023
Accepted 22 August 2023
Published Online 30 December 2023

Keywords
Empagliflozin
Molecular docking
Nephrotoxicity
Network pharmacology
PLAU

Abstract

Guideline-directed medical therapy (GDMT) has been the standard pharmacotherapy for the treatment of HFrEF patients. However, these drugs cause severe side effects like nephrotoxicity. Empagliflozin being a SGLT2 inhibitor has been recently introduced in GDMT, and causes nephrotoxicity to patients. Although, the mechanism how it causes nephrotoxicity is not known. Hence, in the present study, we aimed to utilize system biology tools to predict the potential proteins and pathways responsible for nephrotoxicity. In the present study, we performed network analysis to predict the potential proteins, gene ontology analysis predicted the major cellular components, molecular function and biological process, and molecular docking was performed on empagliflozin with the identified hub genes followed by its validation using molecular dynamic simulations. Network analysis revealed CD44, EGFR, LEP, PLAU, TNFRSF1A, and ATM to be the potential proteins being modulated *via* nuclear factor-kappa B signalling pathway. Molecular docking revealed the empagliflozin-PLAU complex to possess the highest binding affinity of – 8.0 kcal/mol with three hydrogen bond interactions with residues GLN192, ASP194, and SER195. In addition, molecular dynamic simulation studies revealed the empagliflozin-PLAU complex to be stable throughout the MD run with 3-4 consistent hydrogen bonds. Hence, the present study concludes that empagliflozin causes nephrotoxicity in heart failure patients *via* urokinase-type plasminogen activator by regulating the NF-kappa B signalling pathway.

1. Introduction

Heart failure (HF) is one of the major growing disease with an incidence rate of 1% which affects nearly 23 million people worldwide and 80 lakh people in India (Bui *et al.*, 2010; Shahim *et al.*, 2023). For individuals with chronic heart disease, the yearly incidence of HF varies from 0.4% to 2.3% with a mortality of 1-1.6 lakh people in India (Huffman and Prabhakaran, 2010). HF is accidental and is associated with frequent hospitalizations with significant morbidity and death. Ejection fraction determines the kind of heart failure and how it should be treated (Berliner *et al.*, 2020). Patients with an ejection fraction of 40% or less possess left ventricular anatomical abnormalities referred to as patients with reduced ejection fraction (HFrEF) (Dunlay *et al.*, 2017). The current pharmacotherapy of HFrEF involves the use of guideline-directed medical therapy (GDMT) which includes drugs belonging to the categories of angiotensin receptor neprilysin inhibitors (ARNI), angiotensin-converting enzyme inhibitors (ACE-I), angiotensin receptor blockers (ARB), β-blockers (BB), and mineralocorticoid receptor antagonists (MRA) (Joseph *et al.*, 2020; Visseren, 2021). Heart failure is many times diagnosed with multiple comorbidities like obesity and diabetes (Li *et al.*, 2021). For this instance, the European Society of Cardiology (ESC) and the American Heart Association (AHA) jointly have introduced SGLT2 inhibitors in GDMT regimen (Visseren, 2021).

Empagliflozin a SGLT2 inhibitor, is the most commonly used drug in patients with HFrEF alone or with a comorbidity of diabetes mellitus (Liang and Gu, 2022). Empagliflozin since long has been used as a primary drug for the treatment of diabetes as it acts by inhibiting specific proteins in the kidney that reabsorb glucose, therefore causing kidneys to excrete excess glucose *via* urine (Hsia *et al.*, 2017). However, recent advances in its mechanism have displayed empagliflozin to improve heart failure conditions by ameliorating ventricular loading which reduces preload *via* diuretic and natriuretic mechanisms (Pabel *et al.*, 2021). SGLT2 inhibitors function by decreasing the kidneys' ability to reabsorb glucose, which increases the amount of glucose excreted in the urine. This method of action may initially affect kidney function by increasing urine production and slightly decreasing the estimated glomerular filtration rate (eGFR) (Ni *et al.*, 2020). In spite of several advantages of this drug, it has been reported to cause chronic nephrotoxicity in the patients. However, the mechanism by which it causes nephrotoxicity has still not been known (Lin *et al.*, 2019).

Corresponding author: Dr. C. S. Shastry
Professor and Principal, Department of Pharmacy Practice, NGSM Institute of Pharmaceutical Sciences (NGSMIPS), Nitte (Deemed to be University), Mangalore-575018, Karnataka, India
E-mail: principal.ngsmips@nitte.edu.in
Tel.: +91-9731241373

System biology tools have gained importance in recent years and are been utilized for multiple preliminary drug screenings like identifying a novel potential drug, assessing the molecular mechanism, predicting potential molecular targets, and also identifying a lead hit (Khanal *et al.*, 2023; Gezici and Sekeroglu, 2021). In the present study, we have utilized system biology tools like network pharmacology, molecular docking, and gene ontology (GO) analysis to predict potential proteins modulated by empagliflozin which may be the mechanism for nephrotoxicity. For this purpose, we initially identified the proteins known to cause nephrotoxicity and enriched them with the proteins modulated by empagliflozin. A protein-protein interaction network was constructed and KEGG pathways were identified from STRING. The GO analysis was performed to predict the major cellular, molecular, and biological process. Further, the lead hits identified from network analysis (both *via* STRING and Cytoscape) were subjected to molecular docking followed by molecular dynamic simulations and MM_PBSA analysis.

2. Materials and Methods

2.1 Target identification for nephrotoxicity and empagliflozin

The proteins for nephrotoxicity were collected from the DisGeNET database (Piñero *et al.*, 2017; https://www.disgenet.org/) with the keywords "Chronic Kidney Diseases (C1561643)", "Kidney Failure, Chronic (C0022661)", "Kidney Failure, Acute (C0022660)", "hypertensive nephropathy (C0848548)", and "Kidney Diseases (C0022658)", respectively. The targets modulated by empagliflozin were identified using two databases DIGEP-Pred (Lagunin *et al.*, 2013; http://www.way2drug.com/ge/) and SwissTargetPrediction (http://www.swisstargetprediction.ch/) using the retrieved canonical SMILES.

2.2 Network construction, enrichment analysis, and gene ontology analysis

The proteins modulated by empagliflozin and proteins involved in nephrotoxicity were matched and the common proteins were identified. These matched targets were predicted to be concerned in the pathogenesis of nephrotoxicity. The proteins involved in nephrotoxicity were subjected to protein-protein interaction in the STRING (Szklarczyk *et al.*, 2021; https://string-db.org/). In addition, STRING was utilized to identify KEGG-modified pathways and proteins. Further, Cytoscape *ver.* 3.6.1 (Shannon *et al.*, 2003), a java-based tool was used to construct a protein-pathway interaction; the network was analyzed based on "closeness centrality" and "Node degree distribution". The top three proteins identified *via* closeness centrality and node degree distribution were further used for docking. Additionally, the gene ontology was collected from STRING with respect to cellular components, molecular function, and biological process.

2.3 Molecular docking

Molecular docking was performed on six proteins (CD44, EGFR, LEP, PLAU, TNFRSF1A, and ATM) with empagliflozin. Initially, the structure of proteins was queried in the UniProt database (https://www.uniprot.org/) for the presence of targets in the protein databank; the targets for which the structure is not known the proteins were modelled using SWISS MODEL (https://swissmodel.expasy.org/) by inputting the known FASTA sequence. The identified targets were visualized using the discovery studio visualizer and all the hetero atoms were removed followed by energy minimization using 'uff" forcefield. The ligand empagliflozin was retrieved in .sdf format from the PubChem database (https://pubchem.ncbi.nlm.nih.gov/) and was prepared by minimizing its energy using discovery studio visualizer (Santosh *et al.*, 2022; Medhat *et al.*, 2022; Mamta *et al.*, 2022). The targets and ligand empagliflozin were subjected to molecular docking in AutoDock Vina with an exhaustiveness of 8. The binding pocket was initially assessed from the computed atlas of surface topography of proteins 3.0 (CASTp; http://sts.bioe.uic.edu/castp/index.html?1ycs) server. Also, we utilized discovery studio to assess the active site residues. The co-ordinates (center x, center y, center z) and grid size (size x, size y, size z) for protein CD44: -0.51, 1.89, 15.43 and 34.70, 46.94, 47.92, EGFR: 7.95, 42.86, 36.26 and 64.81, 71.85, 81.55, LEP: 226.41, 165.11, 202.61 and 49.61, 31.55, 34.51, PLAU: 22.75,0.18, 31.76 and 58.10, 41.81, 43.71, and TNSRSA1A: 0.21, 27.40, -6.97 and 58.08, 67.18, 68.33, respectively. The protein ATM was not docked due to its excessive size. On completion of molecular docking, the binding energy was analyzed along with the interactions (Shareef and Bhavya, 2021).

2.4 MD simulation and MMPBSA analysis

In the present study, we utilized the gromacs tool version 2022.6 (https://www.gromacs.org/) to perform molecular dynamic simulations. The pdb2gmx module of gromacs was utilized to generate the topology of the protein by implementing the charmm36 forcefield. A three-point water model was utilized to solvate the protein in a dodecahedron box with dimensions of 1 nm^3. Further, sodium (NA^+) and Chloride (Cl^-) ions were added to neutralize the system. Energy minimization was performed for 50,000 steps using the steepest descent integrator with a verlet cutoff scheme. The system was equilibrated using Canonical (NVT) and Isobaric (NPT) for 100 picoseconds. A modified Berendsen thermostat (V-rescale) along with C-rescale was applied to maintain constant volume, temperature at 300 K, and pressure at 1 bar. PME was applied for assessing long-range electrostatics, coulomb, and vander waals with a cut-off of 1.2 nm. The bond length was constrained using the LINCS algorithm. Each complex was subjected to MD run for 50 ns; the coordinates and energies were saved at every 5 picoseconds. The trajectories generated were analyzed using in-built gromacs utilities. In addition, the gmx_MMPBSA module of gromacs was used to analyze the energy contribution per residue and the molecular mechanics.

3. Results

3.1 Target identification for nephrotoxicity and empagliflozin

The SwissTargetPrediction predicted 43 targets with a pharmacological activity greater than 0.1 and DigepPred predicted 20 targets with a Pa>Pi. The DisGeNet database displayed 2314 targets in total to be involved in the development of nephrotoxicity. The 2D and 3D structure of empagliflozin is represented in Figure 1.

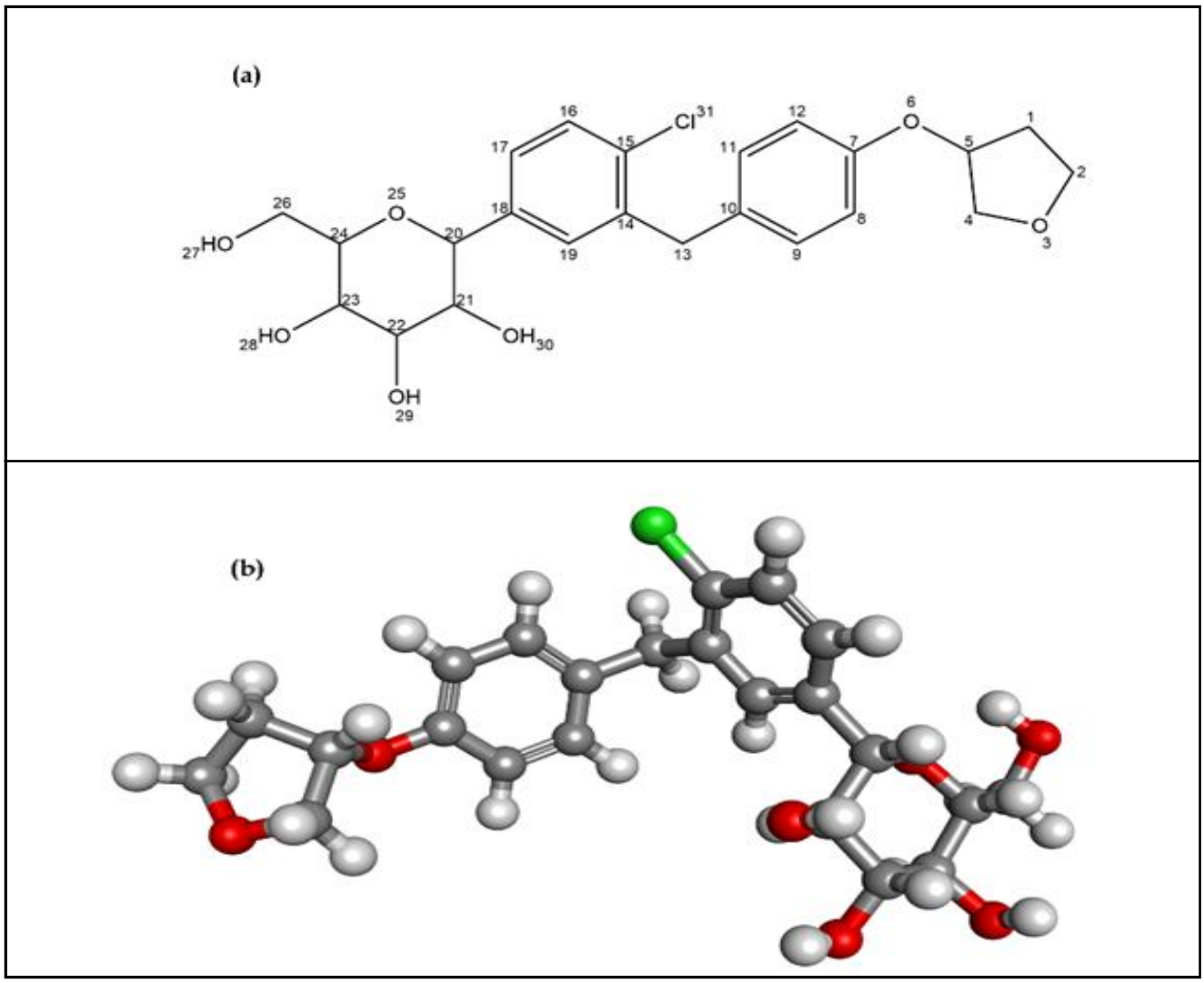

Figure 1: The (a) 2D and (b) 3D structure of empagliflozin (PubChem ID: 11949646); IUPAC name: 2-(4-chloro-3-(4-((tetrahydrofuran-3-yl)oxy)benzyl)phenyl)-6-(hydroxymethyl)tetrahydro-2H-pyran-3, 4, 5-triol, Chemical Formula: $C_{23}H_{27}ClO_7$, molecular weight: 450.91, and InChI Key: OBWASQILIWPZMG-QZMOQZSNSA-N.

3.2 Network construction, enrichment analysis and gene ontology analysis

The enrichment analysis revealed 55% of the proteins modulated by empagliflozin to be present in the pathogenesis of nephrotoxicity (Figure 2). The network analysis *via* string revealed 34 nodes to be present with EGFR to possess the highest node degree of 18 followed by CD44 and LEP with node degrees of 13 and 11, respectively (Figure 3, Table 1). The network was further constructed in cytoscape and was analyzed for closeness centrality which revealed ATM, TNFRSF1A, and PLAU to possess the greatest closeness centrality. The KEGG pathway analysis revealed NF-kappa B signalling pathway (hsa04064) to possess the least false discovery rate of 0.00034 with a strength of 1.46 involving proteins TNFRSF1A, ATM, PLAU, SYK, and CCL4 (Figure 4, Table 2). The gene ontology analysis revealed 12 cellular components in which Extracellular space (GO:0005615) possessed the least false discovery rate of 0.00039 with an observed gene count of 19 (TNFRSF1A, LGALS1, PLAT, CAT, LGALS3, SLC5A1, EGFR, MMP3, LEP, HSPA5, SLC5A2, F3, PLAU, ADIPOQ, CD44, SLC2A1, MME, HSPA8, and CCL4), 9 molecular functions in which D-glucose transmembrane transporter activity (GO:0055056) possessed the least false discovery rate of 0.0103 with an observed gene count of 3 (SLC5A1, SLC5A2, SLC2A1), and 221 biological process in which cellular response to chemical stimulus (GO:0070887) possessed the least false discovery rate of 4.90E-10 with an observed gene count of 24 (TNFRSF1A, PLAT, NR3C1, CAT, LGALS3, EGFR, ATM, MMP3, P2RY12, LEP, NQO1, HSPA5, CYP2B6, F3, ATG5, SYK, ADIPOQ, CD44, SLC2A1, MME, HSPA8, CCL4, SLC29A1, and CYP3A4). These ontology analysis displays that empagliflozin mainly acts on the extracellular space for which it has a molecular function of transferring D-glucose from the transmembrane leading to a chemical response to the body. The top 15 CC, MF, and BP have been represented in Figure 5. The top 3 proteins identified *via* node degree and closeness centrality were further subjected to molecular docking with empagliflozin.

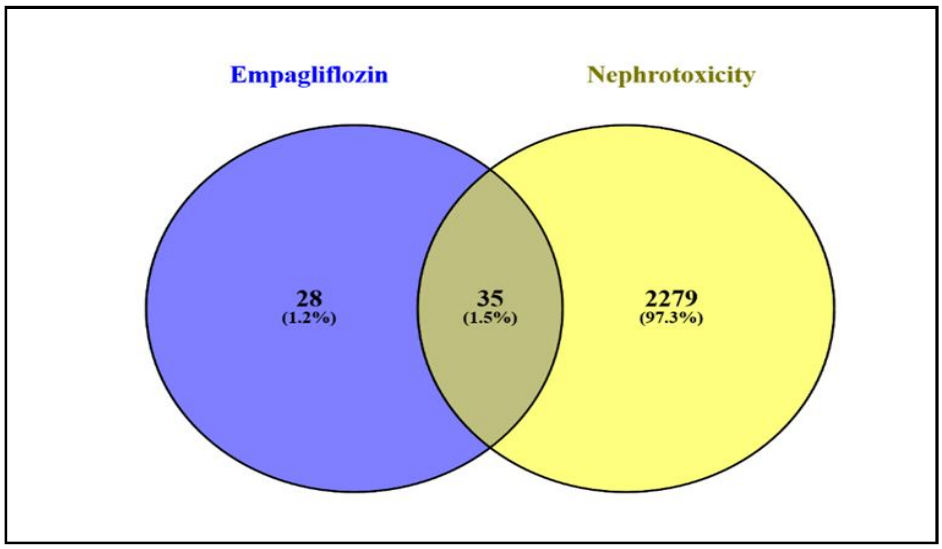

Figure 2: The venn diagram representation of proteins modulated by empagliflozin and proteins involved in nephrotoxicity.

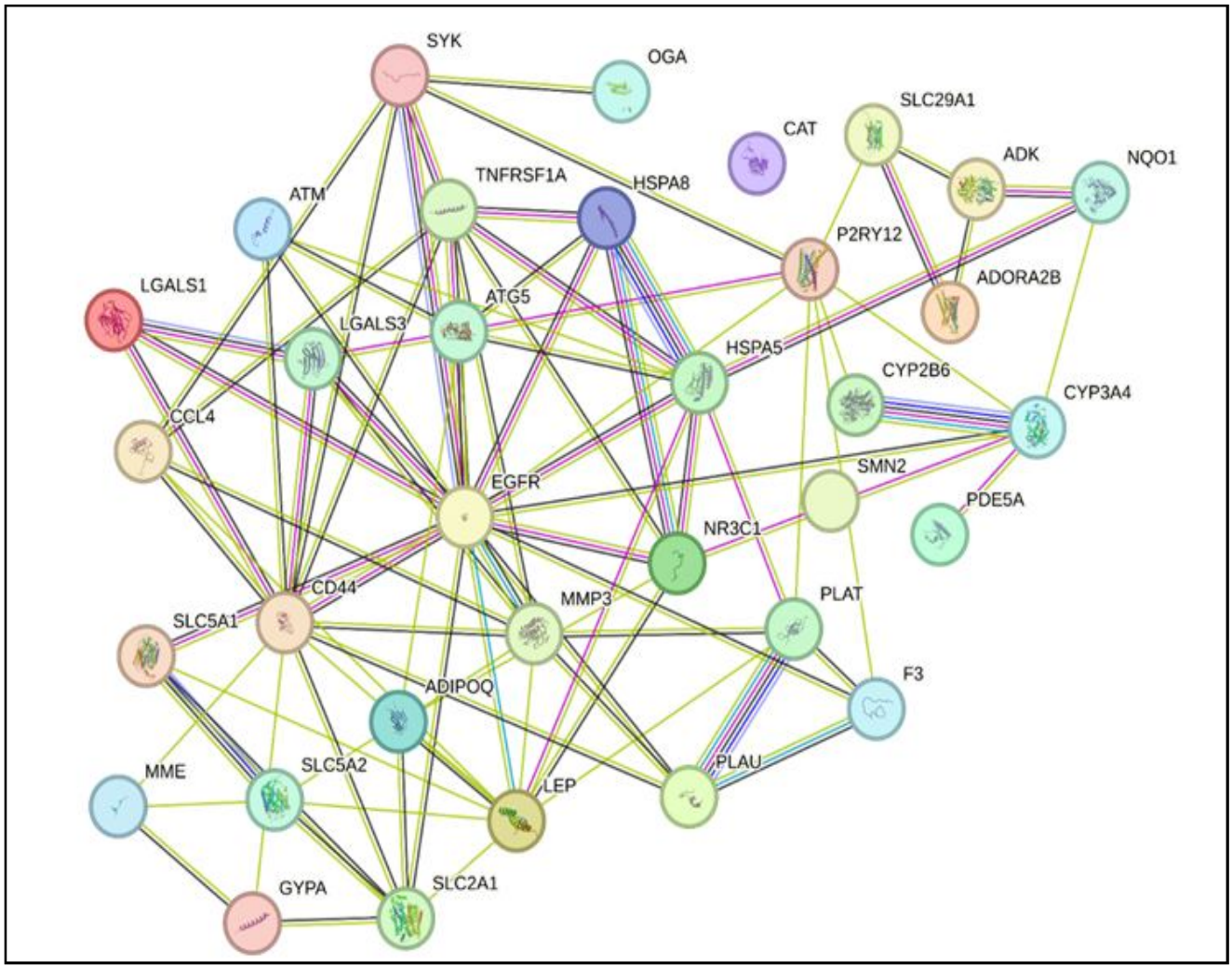

Figure 3: The protein-protein interaction of genes modulated by empagliflozin, involved in nephrotoxicity.

Table 1: The node degree distribution of proteins identified in nephrotoxicity *via* empagliflozin

Low		High	
Protein	**Node degree**	**Protein**	**Node degree**
ADIPOQ	6	F3	4
ADK	3	GYPA	3
ADORA2B	2	HSPA5	9
ATG5	5	HSPA8	5
ATM	4	LEP	11
CAT	0	LGALS1	3
CCL4	5	LGALS3	5
CD44	13	MME	3
CYP2B6	2	MMP3	9
CYP3A4	6	NQO1	3
EGFR	18	NR3C1	7
PLAU	5	OGA	1
SLC29A1	3	P2RY12	8
SLC2A1	7	PDE5A	1
SLC5A1	4	PLAT	6
SLC5A2	5	SYK	6
SMN2	0	TNFRSF1A	8

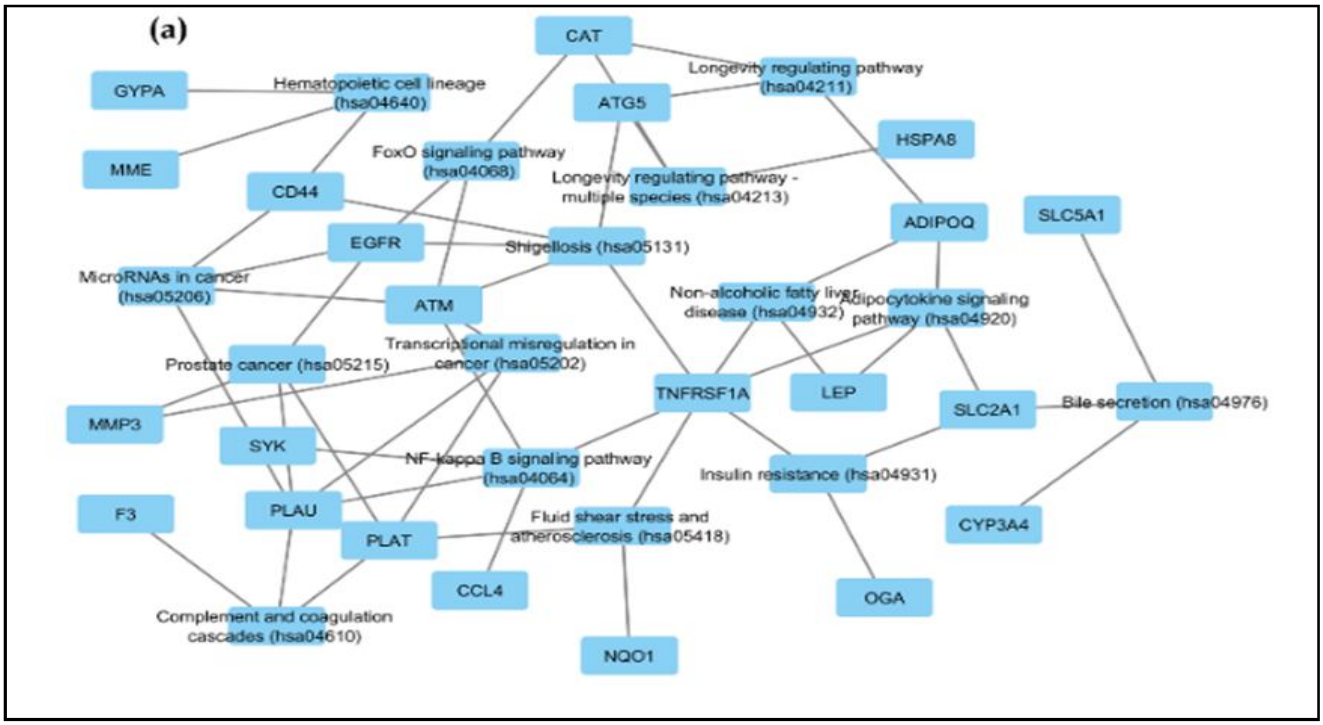

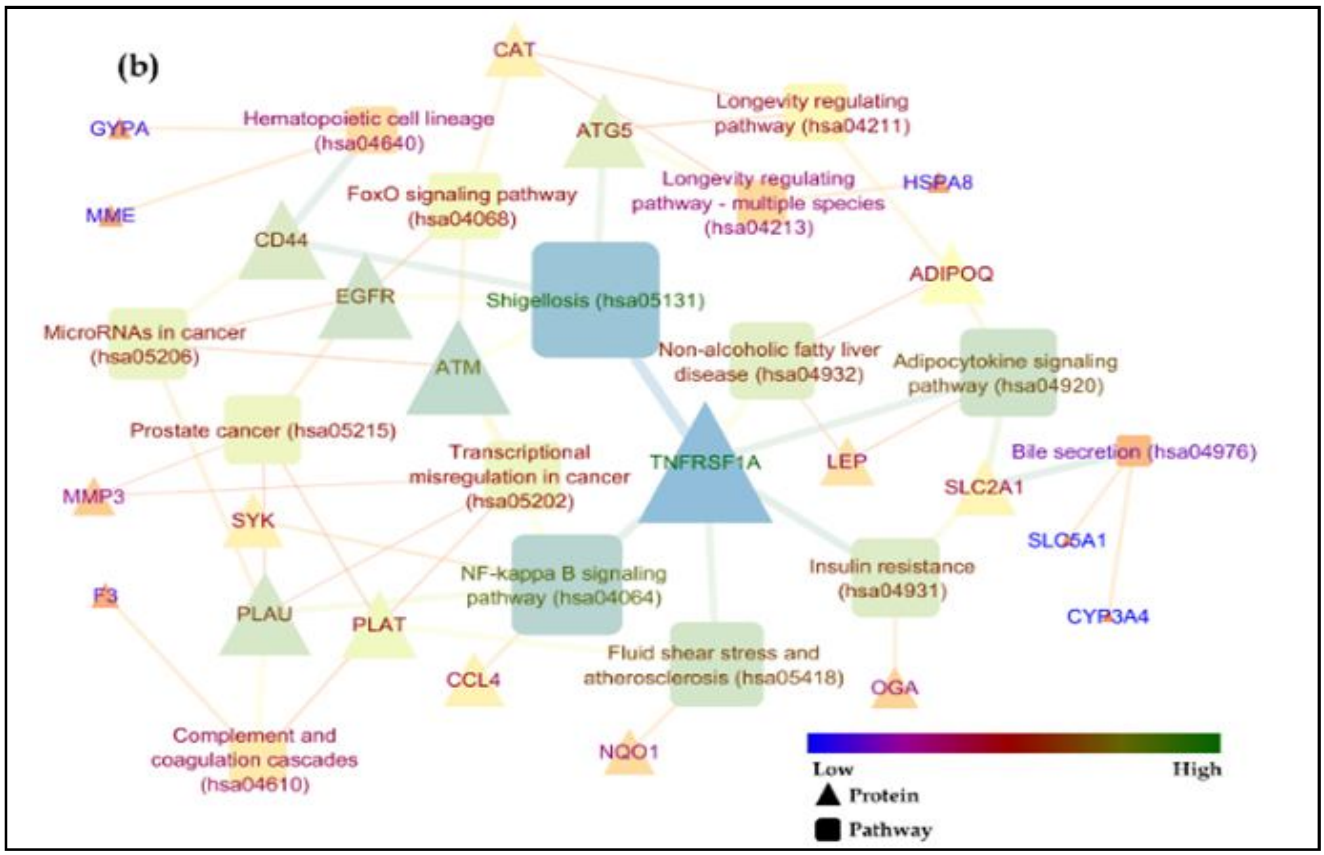

Figure 4: The protein-pathway interaction of genes modulated by empagliflozin involved in nephrotoxicity.

Table 2: The KEGG pathways identified *via* STRING for genes involved in nephrotoxicity by empagliflozin

KEGG ID	Pathway	OGC/BGC	Strength	FDR	Genes
Hsa04064	NF-kappa B signaling pathway	5/101	1.46	0.00034	TNFRSF1A, ATM, PLAU, SYK, CCL4
Hsa04920	Adipocytokine signalling pathway	4/68	1.53	0.0012	TNFRSF1A, LEP, ADIPOQ, SLC2A1
Hsa05215	Prostate cancer	4/97	1.38	0.003	PLAT, EGFR, MMP3, PLAU
Hsa05131	Shigellosis	5/218	1.12	0.0032	TNFRSF1A, EGFR, ATM, ATG5, CD44
Hsa04213	Longevity regulating pathway-multiple species	3/61	1.45	0.0115	CAT, ATG5, HSPA8
Hsa05202	Transcriptional misregulation in cancer	4/171	1.13	0.0115	PLAT, ATM, MMP3, PLAU
Hsa05206	MicroRNAs in cancer	4/159	1.16	0.0115	EGFR, ATM, PLAU, CD44
Hsa04610	Complement and coagulation cascades	3/82	1.33	0.0176	PLAT, F3, PLAU
Hsa04211	Longevity regulating pathway	3/87	1.3	0.0185	CAT, ATG5, ADIPOQ
Hsa04640	Hematopoietic cell lineage	3/90	1.29	0.0185	GYPA, CD44, MME
Hsa04976	Bile secretion	3/88	1.3	0.0185	SLC5A1, SLC2A1, CYP3A4
Hsa04931	Insulin resistance	3/106	1.21	0.0242	TNFRSF1A, OGA, SLC2A1
Hsa04068	FoxO signalling pathway	3/126	1.14	0.0364	CAT, EGFR, ATM
Hsa05418	Fluid shear stress and atherosclerosis	3/129	1.13	0.0364	TNFRSF1A, PLAT, NQO1
Hsa04932	Non-alcoholic fatty liver disease	3/146	1.08	0.0476	TNFRSF1A, LEP, ADIPOQ

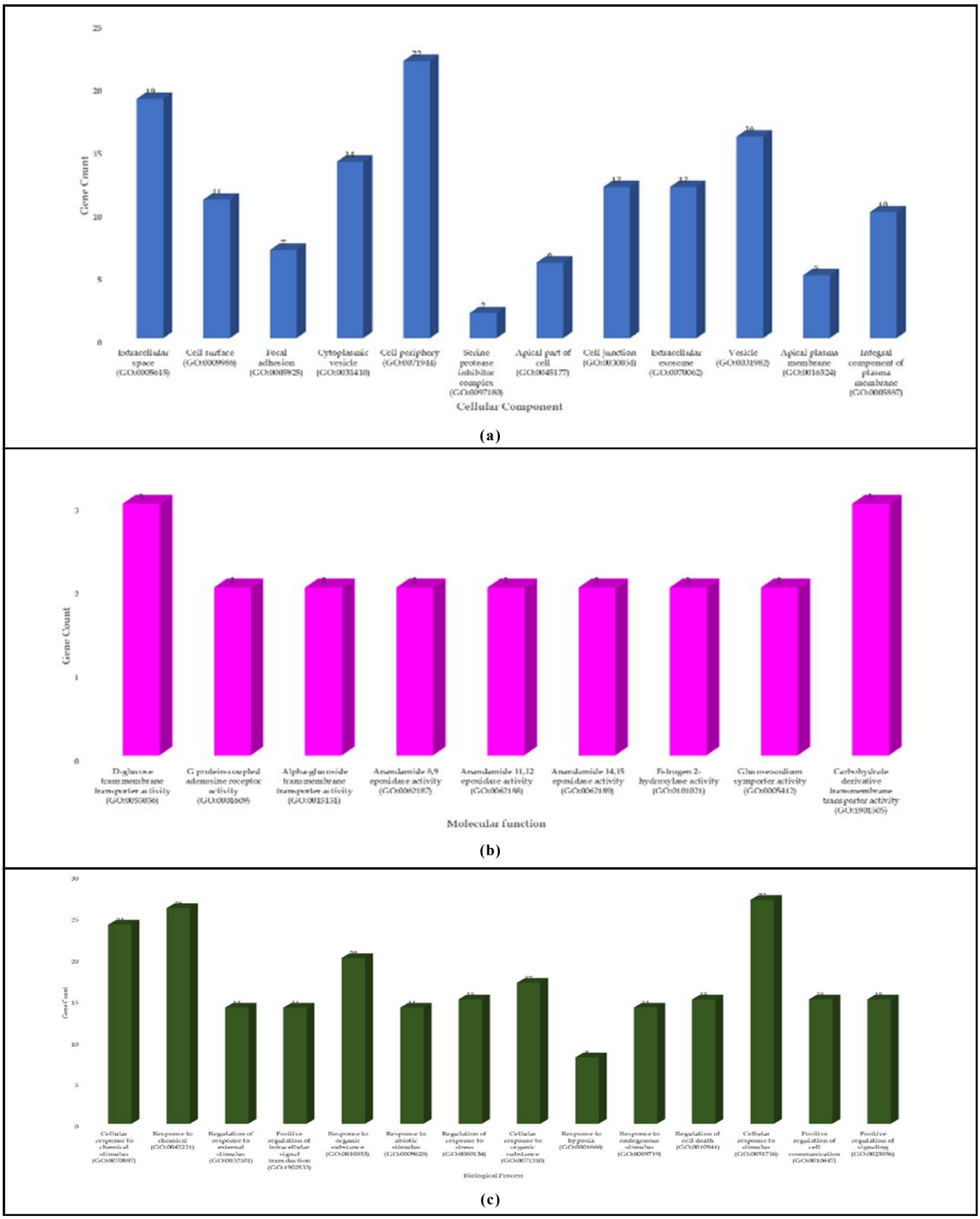

Figure 5: The gene ontology analysis of top 15 GO terms (a) CC: Cellular component, (b) MF: Molecular function, (c) BP: Biological Process.

3.3 Molecular docking

The docking interaction of empagliflozin with PLAU displayed the highest binding affinity with a total energy of -8.0 kcal/mol with 3 hydrogen bond interaction with residues glutamine 192 with the oxygen at position 25, aspartic acid 194 with the hydroxyl atom at position 29, and a carbon-hydrogen bond with residue serine 195; these residues belong to the active site region indicating docking interaction. In addition, 3 π-π bond interactions and 12 vander waal interactions with residues validine 41 and tyrosine 608 and glycine 216, histidine 57, arganine 35, tyrosine 64, cystine 58, tyrosine 151, cystine 191, validine 213, serine 190, serine 214, tryptophan 215, and glycine 193, respectively. The complex empagliflozin-EGFR displayed the second highest binding affinity of -7.5 kcal/mol with 7 hydrogen bond interactions with residues glutamine 8, arginine 405, lysine407, Threonine406, Threonine 378, and glycine 343, 6 π-bond interactions with residues thyronine 406, isoleucine 318, alanine 286, and arganine 285, and 5 vader waal intercation with residues phenylalanine 380, leucine 38, tyrosine 275, glycine 410, and serine 342. The properties of the proteins taken for docking have been depicted in Table 3. The binding energy and interactions of empagliflozin with hub proteins are given in Table 4 and Figure 6 respectively. The docking of empagliflozin with ATM could not be performed as the size of the modelled protein was too large for the software to support.

Table 3: The properties of the top 6 proteins selected for docking with empagliflozin

Protein	Template/PDB ID		Chain	Name	Classification	Resolution (Å)
ATM	7NI5	NA	A	Human ATM kinase with bound inhibitor KU-55933	Signalling protein	2.78
PLAU	NA	1EJN	A	Urokinase plasminogen activator b-chain inhibitor complex	Hydrolase	1.8
TNFRSF1A	NA	1EXT	A	Extracellular domain of the 55kda tumor necrosis factor receptor. crystallized at ph3.7 in p 21 21 21.	Signalling protein	1.85
CD44	NA	1UUH	A	Hyaluronan binding domain of human CD44	Lectin	2.2
EGFR	NA	1MOX	A	Crystal structure of human epidermal Growth factor receptor (residues 1-501) in complex with TGF-alpha	transferase/growth factor	2.5
LEP	8AVE	NA	A	Cryo-EM structure for mouse leptin in complex with the mouse LEP-R ectodomain (1:2 mLEP:mLEPR model).	Cytokine	4.43

Table 4: The docking interaction of empagliflozin with top 6 selected proteins

Protein	BE	NHBD	HBI	NPB	PBI	NVI	VWI
ATM	NA	NA	NA	NA	NA	NA	NA
PLAU	-8	3	GLN192, ASP194, SER195	3	VAL41, TYR608	12	GLY216, HIS57, ARG35, TYR64, CYS58, TYR151, CYS191, VAL213, SER190, SER214, TRP215, GLY193
TNFRSF1A	-6.9	3	SER118, ARG104, GLN102	1	CYS98	0	NA
CD44	-6.6	7	ASN137, TYR161, ASP51, ALA50, THR163	2	LYS54, ALA50	6	ALA138, ALA55, PHE139, SER58, THR59, LEU60
EGFR	-7.5	7	GLN8, ARG405, LYS407, THR406, THR378, GLY343	6	THR406, ILE318, ALA286, ARG285	5	PHE380, LEU38, TYR275, GLY410, SER342
LEP	-6.7	6	SER114, LEU111, LYS32, ASP162	2	GLN28, LYS32	8	SER164, PRO165, ILE24, LYS115, VAL27, THR31, LEU161, LEU158

where, BE (kcal/mol): Binding energy, **NHBD:** Number of hydrogen bond donor, **HBI:** Hydrogen bond interaction, **NPB:** Number of π bonds, **NVI:** Number of Vander Waal forces, and **VWI:** Vander Waal interactions.

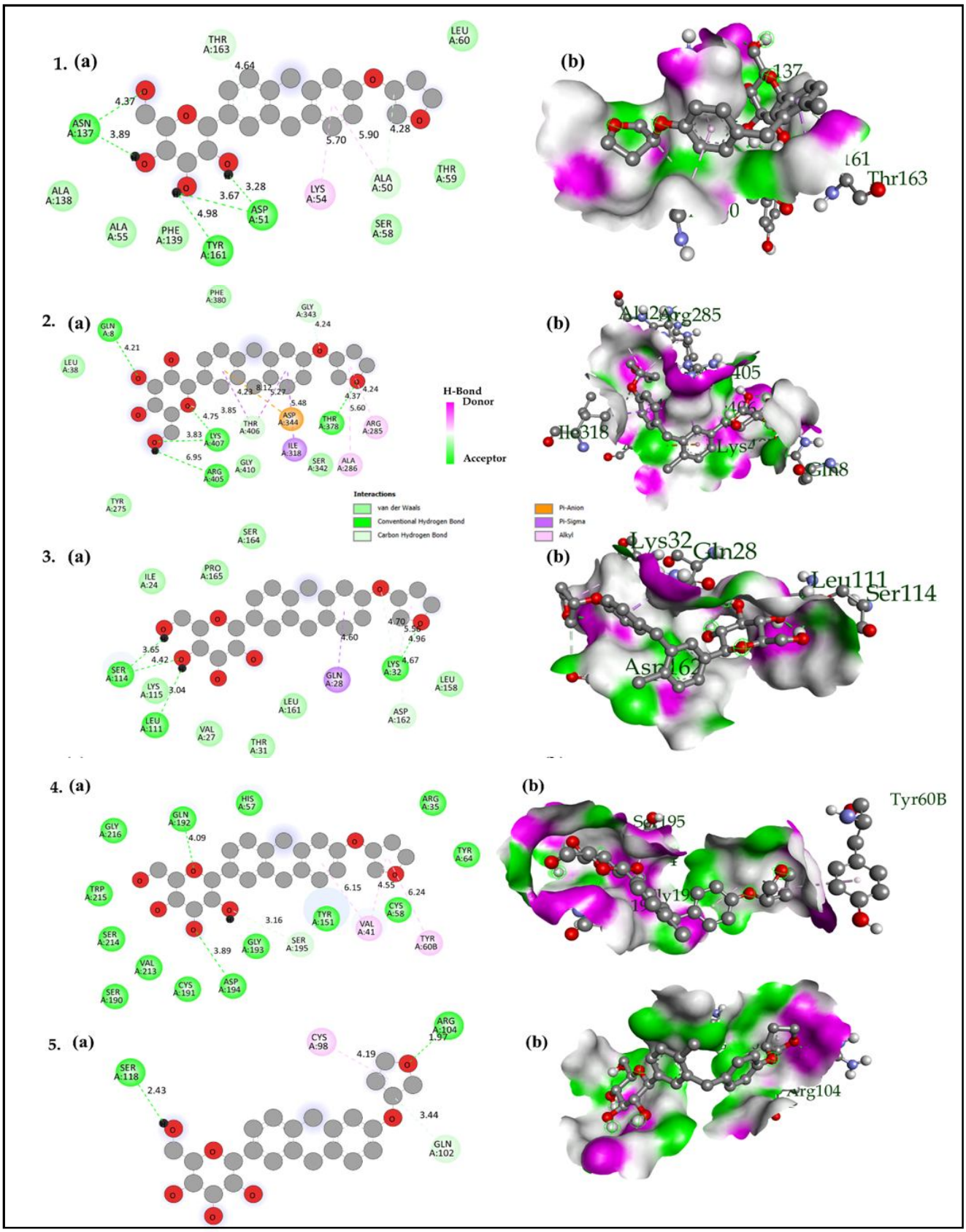

Figure 6: The (a) 2D and (b) 3D docking interaction of 1. CD44, 2. EGFR, 3. LEP, 4. PLAU, 5. TNFRSF1A.

3.4 MD simulation and MMPBSA analysis

The RMSD of the complex and backbone ranged between ~1+Å to ~3+Å throughout the MD run. The difference between the RMSD of the backbone and complex was seen to be ~1+Å. The RMSF of the complex and c-alpha atoms ranged between 0.5 +Å to 5.5 +Å; tyrosine 127 possessed the highest RMSF of 0.32 followed by histidine 37 and methionine with an RMSF of 3.2 +Å and 2.3 +Å (Figure 7). The radius of gyration displays the compactness of the complex which was displayed in the range of ~17.3 +Å to ~17.7 +Å. Similarly, the solvent-accessible surface area was displayed to be in the range of 117 nm^2 to 132 nm^2 (Figure 8). A maximum of 6 hydrogen bonds were visible throughout the MD run from which 3 to 4 bonds were seen to be stable this indicates the stability of the interaction. The total energy decomposition per residue revealed tryptophan 215 to possess the least energy decomposition of – 0.90 kcal/mol followed by serine 195 and isoleucine 16 with energy decomposition of – 0.80 kcal/mol and – 0.69 kcal/mol, respectively. The ligand displayed a total energy contribution of – 8.97 kcal/mol throughout the MD run (Figure 9). The pose of interaction at the start and end of the simulation has been given in Figure 10. The MMPBSA analysis revealed the total relative binding energy for 100 frames for the complex, receptor, ligand and delta to be – 2338.92 ± 6.22 kcal/mol, – 2485.60 ± 6.12 kcal/mol, 138.28 ± 0.75 kcal/mol, and 8.40 ± 0.62 kcal/mol, respectively (Table 5).

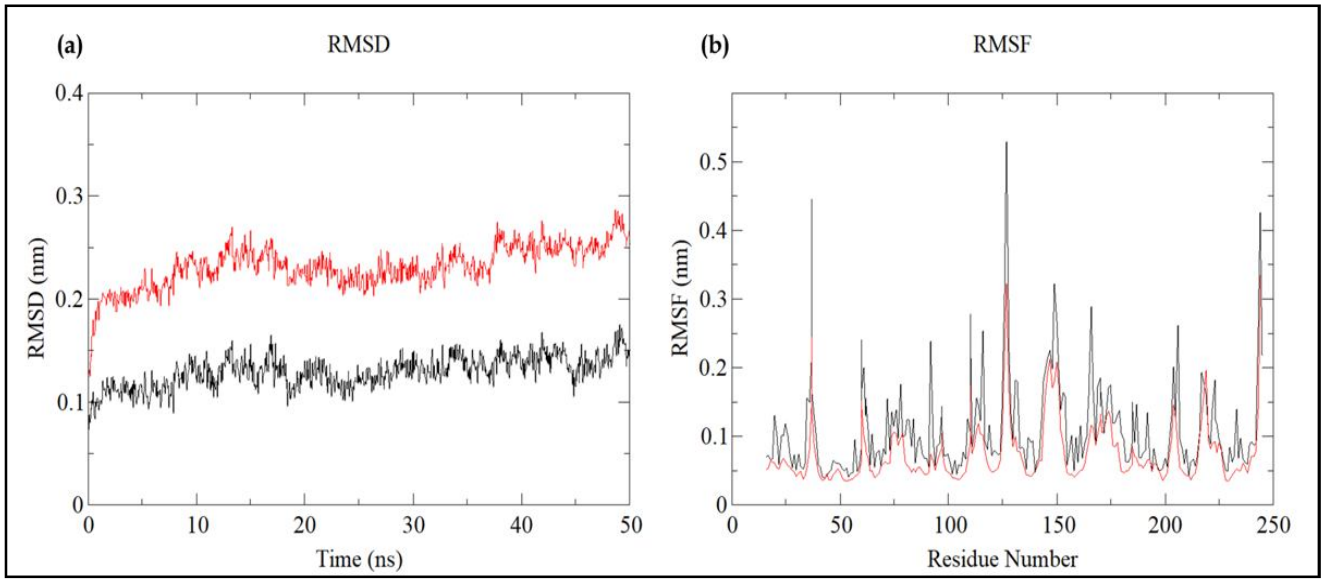

Figure 7: The stability parameters of empagliflozin-PLAU complex (a) the RMSD of the backbone (black) and complex (red); (b) RMSF of the complex (black) and c-alpha atoms (red).

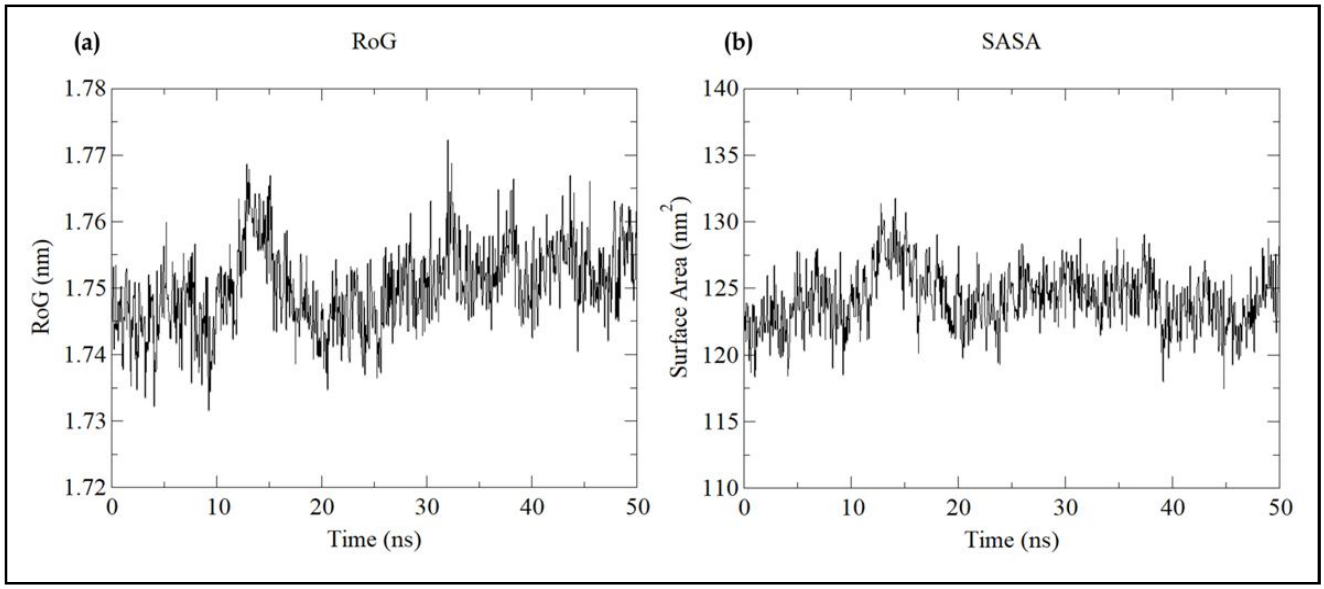

Figure 8: The stability parameters of empagliflozin-PLAU complex. Where, (a) Radius of gyration of the complex and (b) Solvent assessable surface area of the complex.

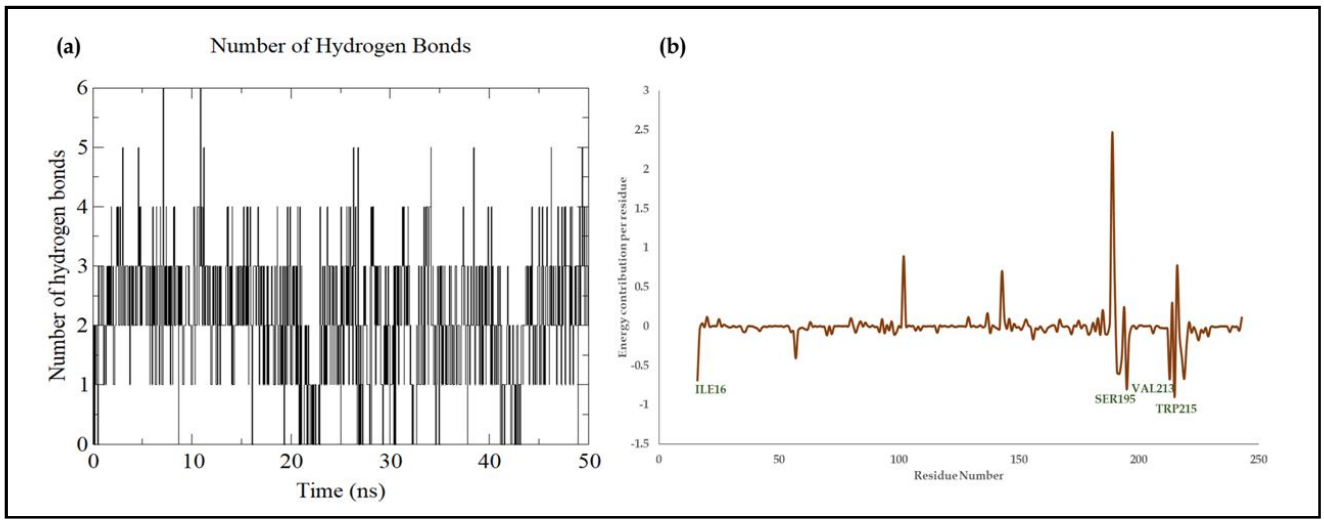

Figure 9: The stability parameters of empagliflozin-PLAU complex. Where, (a) Number of hydrogen bonds; (b) The total energy decomposition per residue.

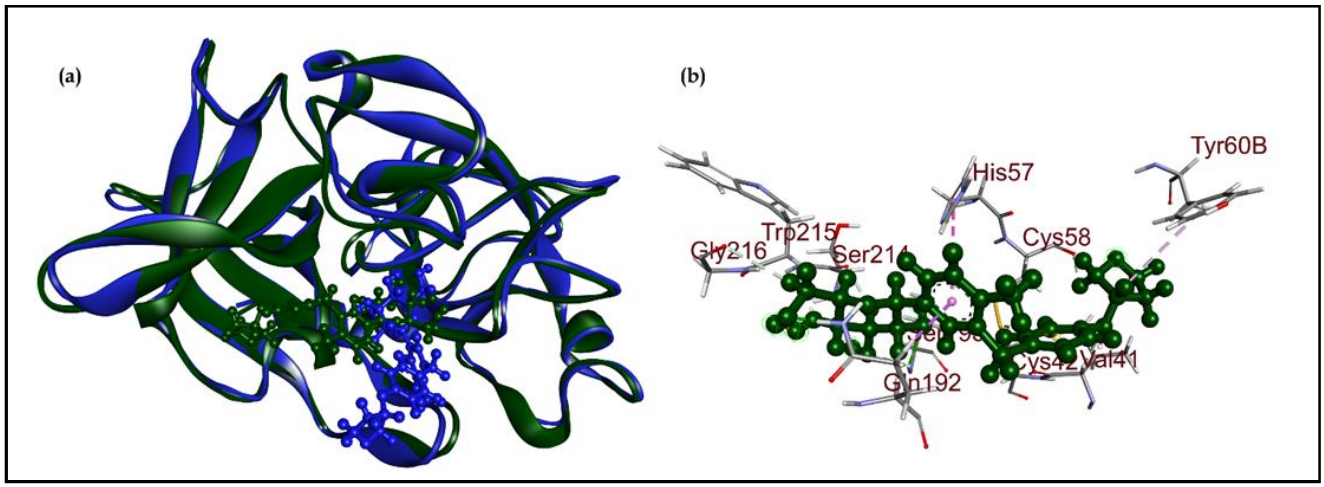

Figure 10: (a) The 3D interaction of empagliflozin-PLAU complex at start (green) and end (blue) of the MD run, (b) The residues interacting with ligand empagliflozin.

Table 5: The MMPBSA analysis of empagliflozin-PLAU complex

Energy component	Complex	Receptor	Ligand	Delta (complex-receptor-ligand)
ΔVDW	– 1760.51 ± 2.28	– 1722.74 ± 2.31	– 3.97 ± 0.23	– 33.80 ± 0.50
ΔEEL	10071.83 ± 7.05	– 14700.66 ± 11.82	– 77.79 ± 0.70	– 19.73 ± 0.76
ΔEPB	– 2868.69 ± 10.75	– 2879.01 ± 10.87	– 31.70 ± 0.30	42.02 ± 0.94
ΔENP	1941.88 ± 1.21	1918.79 ± 1.20	47.61 ± 0.04	– 24.52 ± 0.35
ΔEDISPER	– 1067.84 ± 1.34	– 1067.76 ± 1.25	– 44.52 ± 0.06	44.44 ± 0.47
ΔGGAS	– 344.26 ± 12.28	– 457.61 ± 12.70	166.89 ± 0.75	– 53.54 ± 0.99
ΔGSOL	– 1994.65 ± 10.66	– 2027.98 ± 10.77	– 28.61 ± 0.31	61.94 ± 1.04
ΔGTotal	– 2338.92 ± 6.22	– 2485.60 ± 6.12	138.28 ± 0.75	8.40 ± 0.62

All the data are presented in mean ± SEM where n=100. The unit for each parameter is kcal/mol.

where, " **VDW:** Change in Vander Waals energy; "**EEL:** Electrostatic energy; "**EPB:** Polar contribution to the solvation energy; "**ENP:** Non-polar contribution to solvation energy**;** "**EDISPER:** Non-polar contribution of attractive solute-solvent interactions to the solvation energy; "**GGAS:** Total gas phase energy; "**GSOL:** Total solvation energy; "**GTotal:** Total relative binding energy**.**

4. Discussion

The current advances in the pharmacotherapy of heart failure, by introducing SGLT2 inhibitors in the GDMT for patients diagnosed with HF and diabetes has reduced the drug burden for patients (Keller *et al.*, 2022). This also improves the patient compliance with the drugs. It is reported that patients with either heart failure or diabetes undergo long-term medications which has been reduced by including SGLT2 inhibitors in the GDMT dosage regimen by the ESC and AHA (Greenberg, 2022). This change in the regimen has resulted in empagliflozin being the first choice of drug for patients diagnosed with diabetes and heart failure (Kowalska *et al.*, 2021). However, empagliflozin has been reported to cause severe nephrotoxicity in some patients; the mechanism by which it causes nephrotoxicity is still unclear (Nadkarni *et al.*, 2017). Hence, it encouraged us to identify the potential targets how empagliflozin causes nephrotoxicity. For this, we utilized a combination of computational biology tools like network pharmacology, GO analysis, molecular docking and molecular dynamic simulation.

The network analysis revealed that the proteins CD44, EGFR, LEP, PLAU, and TNFRSF1A as the hub genes, which were further confirmed *via* molecular docking and the top complex was selected for molecular dynamic simulations. The ontology analysis displays that empagliflozin mainly acts on the extracellular space for which it has a molecular function of transferring D-glucose from the transmembrane leading to a chemical response to the body. This indicates that the biological response is taking place in the extracellular space which leads to a chemical response and modulates PLAU and EGFR proteins in the cell. The docking interaction can be visualized to be stable with multiple hydrogen bond interactions indicating a biological response which is undesired. Molecular dynamic simulations confirmed the complex empagliflozin-PLAU to be stable throughout the MD run this confirms the interaction of empagliflozin with plasminogen activator, Urokinase (PLAU). PLAU is produced by the Proximal and distal tubular epithelial cells which is then released through the apical membrane and into the urine area, other sources of PLAU include monocytes/macrophages, fibroblasts and myofibroblasts (Zhang and Eddy, 2008). For decades, there has been interest in the function of fibrinolytic pathways in the pathophysiology of acute glomerular illness (Przybyciński *et al.*, 2021). Until recently, the role of PLAU in chronic kidney diseases has been unknown. However, recent research displays elevated levels of PLAU in experimental models of chronic kidney disease induced by unilateral ureteral ligation (Martínez-Klimova *et al.*, 2019). PLAU does not seem to be expressed in healthy kidneys, according to studies on mRNA expression in mice. However, in human renal disorders such as diabetic nephropathy, allograft rejection, and pyelonephritis there has been a confirmation of *denovo* expression by glomerular and tubular epithelial cells (Zhang and Eddy, 2008).

Our results have displayed NF-kappa B signalling pathway to be the major pathway being modulated by empagliflozin to cause nephrotoxicity. NF-kappa B and PLAU have been known to possess a significant role in cell apoptosis and cancers (Brown *et al.*, 2008). Nuclear factor kappa B is essential for several biological processes such as immunological response, inflammation, cell growth and survival (Park and Hong, 2006). Our results displayed PLAU as the major protein modulated *via* empagliflozin which may be through the NF-kappa B signalling pathway. Hence the present study reports that empagliflozin causes nephrotoxicity in patients by the modulation of Plasminogen activator urokinase which is regulated through the nuclear factor kappa B signalling pathway. However, the present study involves the use of *in silico* tools which needs to be validated by experimental protocols.

5. Conclusion

The present study concludes that empagliflozin causes nephrotoxicity in heart failure patients *via* the modulation of Plasminogen Activator, Urokinase (PLAU) which may be through the nuclear factor kappa B signalling pathway. These results have been retrieved *via* system biology tools which need to be validated through wet lab protocols, this is the future scope as well as drawback of the present study.

List of abbreviations

ACE: Angiotensin converting enzyme inhibitor; **AHA:** American Heart Association; **ARB:** Angiotensin receptor blocker; **ARNI:** Angiotensin receptor-nelprilysin inhibitor; **BB:** Beta blockers; **CKD:** Chronic kidney disease ; **EF:** Ejection fraction; **ESC:** European Society of Cardiology; **GDMT:** Guideline Directed Medical Therapy; **HF:** Heart failure; **HFrEF:** Heart Failure with reduced ejection fraction; **KEGG:** Kyoto encyclopedia of genes and genomes; **MD:** Molecular dynamics; **MMPBSA:** Molecular Mechanics Poisson-Boltzmann Surface Area; **MRA:** Mineralocorticoid receptor antagonists; **Pa:** Pharmacological activity; **Pi:** Pharmacological inactivity; **PDB:** Protein data bank; **RMSD:** Root Mean Square Deviation; **RMSF:** Root Mean Square Fluctuation; **RoG:** Radius of Gyration; **SASA:** Solvent Assessable Surface Area; **SGLT2:** Sodium-glucose Cotransporter-2.

Acknowledgements

The authors are thankful to NGSM Institute of Pharmaceutical Sciences for the smooth conduct of this research.

Conflict of interest

The authors declare no conflict of interest relevant to this article.

References

Berliner, D.; Hänselmann, A. and Bauersachs, J. (2020). The treatment of heart failure with reduced ejection fraction. Dtsch Arztebl Int., **117**(21):376-386. https://doi.org/10.3238/arztebl.2020.0376.

Brown, M.; Cohen, J.; Arun, P.; Chen, Z. and Van Waes, C. (2008). NF-kappaB in carcinoma therapy and prevention. Expert Opin Ther Targets., **12**(9):1109-22. https://doi.org/10.1517/14728222.12.9.1109.

Bui, A.L.; Horwich, T.B. and Fonarow, G.C. (2011). Epidemiology and risk profile of heart failure. Nat. Rev. Cardiol., **8**(1):30-41. https://doi.org/10.1038/nrcardio.2010.165.

Dunlay, S.M.; Roger, V.L. and Redfield, M.M. (2017). Epidemiology of heart failure with preserved ejection fraction. Nat. Rev. Cardiol., **14**(10):591-602. https://doi.org/10.1038/nrcardio.2017.65.

Gezici, S. and Sekeroglu, N. (2021). Network-based bioinformatics analyses on molecular pathways and pharmacological properties of oleuropein. Ann. Phytomed., **10**(2):223-232. http://dx.doi.org/10.21276/ap.2021.10.2.31

Greenberg, B. (2022). Medical management of patients with heart failure and reduced ejection fraction. Korean Circ. J., **52**(3):173-197. https://doi.org/10.4070/kcj.2021.0401.

Hsia, D.S.; Grove, O. and Cefalu, W.T. (2017). An update on sodium-glucose co-transporter-2 inhibitors for the treatment of diabetes mellitus. Curr. Opin. Endocrinol Diabetes Obes., **24**(1):73-79. https://doi.org/10.1097/MED.0000000000000311.

Huffman, M.D. and Prabhakaran, D. (2010). Heart failure: Epidemiology and prevention in India. Natl. Med. J. India, **23**(5):283-288.

Joseph, J.; PP, S.; James, J. and Abraham, S. (2020). Abdullakutty J. Guideline-directed medical therapy in heart failure patients: impact of focused care provided by a heart failure clinic in comparison to general cardiology out-patient department. Egypt Heart J., **72**(1):53. https://doi.org/10.1186/s43044-020-00088-8.

Keller, D.M.; Ahmed, N.; Tariq, H.; Walgamage, M.; Walgamage, T.; Mohammed, A.; Chou, J.T.; Ka³u¿na-Oleksy, M.; Lesiak, M. and Straburzyñska-Migaj, E. (2022). SGLT2 inhibitors in type 2 diabetes mellitus and heart failure: A concise review. J. Clin. Med., **11**(6):1470. https://doi.org/10.3390/jcm11061470.

Khanal, P.; Patil, V.S.; Bhandare, V.V.; Patil, P.P.; Patil, B.M.; Dwivedi, P.S.R.; Bhattacharya, K.; Harish, D.R. and Roy, S. (2023). Systems and *in vitro* pharmacology profiling of diosgenin against breast cancer. Front Pharmacol., **13**:1052849. https://doi.org/10.3389/fphar. 2022.1052849.

Kowalska. K.; Walczak, J.; Femlak, J.; M³ynarska, E.; Franczyk, B. and Rysz, J. (2021). Empagliflozin: A new chance for patients with chronic heart failure. Pharmaceuticals (Basel)., **15**(1):47. https://doi.org/10.3390/ph15010047.

Lagunin, A.; Ivanov, S.; Rudik, A.; Filimonov, D. and Poroikov, V. (2013). DIGEP-Pred: Web service for *in silico* prediction of drug-induced gene expression profiles based on structural formula. Bioinformatics., **29**(16):2062-3. https://doi.org/10.1093/bioinformatics/btt322.

Li, Z.; Zhao, H. and Wang, J. (2021). Metabolism and chronic inflammation: the links between chronic heart failure and comorbidities. Front Cardiovasc Med., **8**:650278. https://doi.org/10.3389/fcvm.2021.650278.

Liang, B. and Gu, N. (2022). Empagliflozin in the treatment of heart failure and type 2 diabetes mellitus: Evidence from several large clinical trials. Int. J. Med. Sci., **19**(7):1118-1121. https://doi.org/10.7150/ijms.72772.

Lin, Y.H.; Huang, Y.Y.; Hsieh, S.H.; Sun, J.H.; Chen, S.T. and Lin, C.H. (2019). Renal and glucose-lowering effects of empagliflozin and dapagliflozin in different chronic kidney disease stages. Front Endocrinol (Lausanne)., **10**:820. https://doi.org/10.3389/fendo.2019.00820.

Mamta A.; Rathour, K.S.; Tiwari A.; Chauhan V.S. and Taj G. (2022). Molecular docking studies of COX-2 protein with 8-deoxylactucin of *Cichorium intybus* L. involved in anti-inflammation activity. Ann. Phytomed., **11**(1):371-375. http://dx.doi.org/10.54085/ap.2022.11.1.41.

Martínez-Klimova, E.; Aparicio-Trejo, O.E. and Tapia, E. (2019). Pedraza-chaverri J. unilateral ureteral obstruction as a model to investigate fibrosis-attenuating treatments. Biomolecules, **9**(4):141. https://doi.org/10.3390/biom9040141.

Medhat, F.; Aslam, P. and Nawaf A. (2022). Molecular docking analysis of ten plant products for the inhibition of spike glycoprotein and prospective use as anti-COVID compounds. Ann. Phytomed., **11**(2):302-308. http://dx.doi.org/10.54085/ap.2022.11.2.35.

Nadkarni, G.N.; Ferrandino, R.; Chang, A.; Surapaneni, A.; Chauhan, K.; Poojary, P.; Saha, A.; Ferket, B.; Grams, M.E. and Coca, S.G. (2017). Acute kidney injury in patients on SGLT2 inhibitors: A propensity-matched analysis. Diabetes Care, **40**(11):1479-1485. https://doi.org/10.2337/dc17-1011.

Ni, L.; Yuan, C.; Chen, G.; Zhang, C. and Wu, X. (2020). SGLT2i: Beyond the glucose-lowering effect. Cardiovasc Diabetol., **19**(1):98. https://doi.org/10.1186/s12933-020-01071-y.

Pabel, S.; Hamdani, N.; Luedde, M. and Sossalla, S. (2021). SGLT2 inhibitors and their mode of action in heart failure-has the mystery been unravelled? Curr. Heart Fail Rep., **18**(5):315-328. https://doi.org/10.1007/s11897-021-00529-8.

Park, M.H. and Hong, J.T. (2016). Roles of NF-κB in cancer and inflammatory diseases and their therapeutic approaches. Cells, **5**(2):15. https://doi.org/10.3390/cells5020015.

Piñero, J., Bravo, A., Queralt-Rosinach, N., Gutiérrez-Sacristán, A., Deu-Pons, J., Centeno, E.; García-García, J.; Sanz, F. and Furlong, L.I. (2017). DisGeNET: A comprehensive platform integrating information on human disease-associated genes and variants. Nucleic Acids Res., **45**(D1):D833-D839. https://doi.org/10.1093/nar/gkw943.

Przybyciñski, J.; Dro¿d¿al, S.; Domañski, L.; Dziedziejko, V. and Pawlik, A. (2021). Role of endothelial glucocorticoid receptor in the pathogenesis of kidney diseases. Int. J. Mol. Sci., **22**(24):13295. https://doi.org/10.3390/ijms222413295.

Puri, T.S.; Shakaib, M.I.; Chang, A.; Mathew, L.; Olayinka, O.; Minto, A.W.; Sarav, M.; Hack, B.K. and Quigg, R.J. (2010). Chronic kidney disease induced in mice by reversible unilateral ureteral obstruction is dependent on genetic background. Am. J. Physiol. Renal. Physiol., **298**(4):F1024-32. https://doi.org/10.1152/ajprenal.00384.2009.

Santosh, K.; Sanjeev, P.; Sonia, Y. and Yadav, D.K. (2022). Network pharmacology-based validation of traditional therapeutic claim of *Boerhavia diffusa* L. in the alleviation of kidney dysfunction. Ann. Phytomed., **11**(2):351-359. http://dx.doi.org/10.54085/ap.2022.11.2.42.

Shahim, B.; Kapelios, C.J.; Savarese, G. and Lund, L.H. (2023). Global public health burden of heart failure: An updated review. Card. Fail Rev., **9**:e11. https://doi.org/10.15420/cfr.2023.05.

Shannon, P.; Markiel, A.; Ozier, O.; Baliga, N.S.; Wang, J.T.; Ramage, D.; Amin, N.; Schwikowski, B. and Ideker, T. (2003). Cytoscape: A software environment for integrated models of biomolecular interaction networks. Genome Res., **13**(11):2498-504. https://doi.org/ 10.1101/gr.1239303.

Shareef, M.M. and Bhavya E. (2021). Extraction, phytochemical analysis and *in silico* antidepressant studies of aqueous extract of leaves of *Hibiscus sabdariffa* L. Ann. Phytomed., **10**(2):448-455. http://dx.doi.org/10.21276/ap.2021.10.2.59.

Szklarczyk, D.; Gable, A.L.; Nastou, K.C.; Lyon, D.; Kirsch, R.; Pyysalo, S.; Doncheva ,N.T.; Legeay, M.; Fang, T.; Bork, P.; Jensen, L.J. and von Mering, C. (2021). The STRING database in 2021: Customizable protein-protein networks, and functional characterization of user-uploaded gene/measurement sets. Nucleic Acids Res., **49**(D1):D605-D612. https://doi.org/10.1093/nar/gkaa1074.

Visseren, F.L.J. (2021). 2021 ESC guidelines on cardiovascular disease prevention in clinical practice. Eur. Heart J., **42**(34):3227-3337. https://doi.org/10.1093/eurheartj/ehab484.

Zhang, G. and Eddy, A.A. (2008). Urokinase and its receptors in chronic kidney disease. Front Biosci., **13**:5462-5478. https://doi.org/10.2741/3093.

Citation **Anu Philip, Prarambh S R Dwivedi, C. S. Shastry and Basavaraj Utagi (2023). Empagliflozin causes nephrotoxicity in patients on Guideline-directed medical therapy *via* urokinase-type plasminogen activator: An *in silico* approach. Ann. Phytomed., 12(2):607-619. http://dx.doi.org/10.54085/ap.2023.12.2.71.**